Biomechanics and Modeling in Mechanobiology
https://doi.org/10.1007/s10237-022-01565-6

ORIGINAL PAPER

Inhibiting the β1integrin subunit increases the strain threshold for neuronal dysfunction under tensile loading in collagen gels mimicking innervated ligaments

Sagar Singh[1] · **Beth A. Winkelstein**[1,2]

Received: 21 February 2021 / Accepted: 13 February 2022
© The Author(s), under exclusive licence to Springer-Verlag GmbH Germany, part of Springer Nature 2022

Abstract
Stretch injury of the facet capsular ligament is a cause of neck pain, inducing axonal injury, neuronal hyperexcitability, and upregulation of pain neuromodulators. Although thresholds for pain and collagen reorganization have been defined and integrins can modulate pain signaling with joint trauma, little is known about the role of integrin signaling in neuronal dysfunction from tensile loading of the innervated capsular ligament. Using a well-characterized biomimetic collagen gel model of the capsular ligament's microstructure and innervation, this study evaluated extrasynpatic expression of N-Methyl-D-Aspartate receptor subtype 2B (NR2B) as a measure of neuronal dysfunction following tensile loading and determined mechanical thresholds for its upregulation in primary sensory neurons, with and without integrin inhibition. Collagen gels with dissociated dorsal root ganglion neurons ($n=16$) were fabricated; a subset of gels ($n=8$) was treated with the β1 integrin subunit inhibitor, TC-I15. Gels were stretched to failure in tension and then immunolabeled for axonal NR2B. Inhibiting the integrin subunit does not change the failure force ($p=0.12$) or displacement ($p=0.44$) but does reduce expression of the β1 subunit by 41% ($p<0.001$) and decrease axonal NR2B expression after stretch ($p=0.018$). Logistic regressions estimating the maximum principal strain threshold for neuronal dysfunction as evaluated by Analysis of Covariance determine that integrin inhibition increases ($p=0.029$) the 50th percentile strain threshold (7.1%) above the threshold for upregulation in untreated gels (6.2%). These results suggest that integrin contributes to stretch-induced neuronal dysfunction via neuron–integrin–collagen interactions.

Keywords Axonal injury · Ligament · Integrin · Mechanotransduction

1 Introduction

Neuronal injury and/or dysfunction can occur by mechanical deformation, even at magnitudes below those producing axonal damage or failure (Hemphill et al. 2015; Hill et al. 2016). Macroscopic loading of neuron-dense tissue can directly deform neurons and produce morphological changes to their axonal cytoskeleton, impairing protein transport and action potential transmission (Laplaca and Thibault 1998; Tang-Schomer et al. 2010, 2012; Tekieh et al. 2016). Indeed, for joint capsular ligaments in which neurons are embedded in a surrounding collagen network, forces are transmitted through the surrounding matrix and mechanotransduction is primarily mediated by the integrins (Chen et al. 1999; Hoffman et al. 2011; Kong et al. 2013; Janoštiak et al. 2014; Sun et al. 2016). Integrins are transmembrane receptors that facilitate adhesion between cells and the extracellular matrix (Müller 2004), with a host of integrin subunits expressed on the membrane surface, depending on cell type and the surrounding matrix composition (Hynes 2002; Sun et al. 2016, 2019). Integrin signaling is one of the main mechanotransduction pathways through which cells sense changes to their extracellular environment (Hoffman et al. 2011; Stukel and Willits 2016). Matrix deformations can activate integrins, leading to, among other things, the intracellular release and expression of cytokines and activation of other signaling transduction pathways via MAP kinases, including the upregulation and transport of transmembrane ion

✉ Beth A. Winkelstein
winkelst@seas.upenn.edu

[1] Department of Bioengineering, University of Pennsylvania, 210 S. 33rd St, Philadelphia, PA 19104, USA

[2] Department of Neurosurgery, University of Pennsylvania, 3400 Spruce St, Philadelphia, PA 19104, USA

Published online: 12 March 2022

channels (Dina et al. 2005; Wiesner et al. 2005; Lal et al. 2007; Hemphill et al. 2011; Wu and Reddy 2012; Hamidi and Ivaska 2018). Although these events are known to initiate further downstream cascades that activate transcription factors associated with cellular injury and regeneration (Hunt et al. 2012; Chang et al. 2019), less is known about how integrin incites neuronal dysfunction.

The spinal facet capsular ligament is composed of collagen and elastin fibers and innervated by primary afferent nerve fibers that have their cell bodies in the dorsal root ganglia (DRG) (Cavanaugh et al. 1996; Yamashita et al. 1996; Kallakuri et al. 2012). Excessive facet capsular stretch has been identified as a cause of neck pain from whiplash injury and cervical trauma (Lee et al. 2004a, b, 2006a; Cavanaugh 2006; Yoganandan et al. 2008; Quinn et al. 2010b; Dong et al. 2012). During stretch, collagen fibers deform and realign, transmitting forces to the neurons interspersed in the matrix (Quinn et al. 2010a; Zarei et al. 2017a, b). In vivo and ex vivo approaches have elucidated the biomechanical and neurophysiological mechanisms of pain and injury and have defined thresholds for mechanical events in the tissue, pain onset, tissue damage and failure, and mechanisms of central sensitization that maintains pain (Lee et al. 2004a, b, 2006a; Quinn et al. 2007, 2010b; Dong et al. 2012; Kras et al. 2013; Crosby et al. 2014). Ex vivo studies of subfailure loading of the facet capsule of the rat and the human cadaver that generate mechanical tissue-level strains that induce fiber-scale collagen realignment and anomalous ligament network reorganization are also associated with pain and neuronal hyperexcitability in vivo (Quinn and Winkelstein 2010, 2011a, b; Quinn et al. 2010a; Dong et al. 2012). Despite identifying such biomechanical thresholds for altered collagen fiber behavior in the context of stretch-induced pain, less is known about those mechanical thresholds for inducing neuronal dysfunction and/or functional injury.

Integrins are expressed in primary sensory neurons as a heterodimer composed of the α2 and β1 subunits (Khalsa et al. 2000; Dina et al. 2004; Malik-Hall et al. 2005; Al-Jamal and Harrison 2008). Besides facilitating adhesion of the neuronal cytoskeleton to the surrounding collagen matrix, the β1 subunit modulates neuronal excitability, and is activated by noxious stretch (Emsley et al. 2000; Hynes 2002; Sun et al. 2019). One of the mechanisms responsible for neuronal hyperexcitability is the upregulation of extrasynaptic N-methyl-D-aspartate (NMDA) receptor, a transmembrane glutamate receptor and Ca^{2+} channel protein (Petralia et al. 2009; Gladding and Raymond 2011). NMDA receptors predominantly express the N-Methyl-D-aspartate receptor subunit 2A (NR2A), subunit 2B (NR2B), or both, subunits depending on where on the neuron the receptors are expressed (Li et al. 1998; Grossman et al. 2000; Groc et al. 2006; Petralia et al. 2009). NMDA receptors located at the synaptic cleft express both the NR2A and NR2B subunits, whereas extrasynaptic or axonal NMDA receptors primarily express NR2B (Li et al. 1998; Petralia et al. 2009; Unezaki et al. 2012). Transport of NR2B containing NMDA receptors to extrasynaptic regions of the neuron has been shown to be mediated by the activation of the β1 integrin subunit in hippocampal neurons (Groc et al. 2006, 2007; Ladépêche et al. 2014) and in the periphery (Wigerblad et al. 2017). But whether and how this change in receptor population and/or localization is mediated by the kinematics of the surrounding matrix in ligament tissue is not known.

Although mechanical thresholds have been defined for pathophysiological outcomes in the facet capsular ligament in vivo (Lee et al. 2006a; Quinn and Winkelstein 2007; Quinn et al. 2010a; Crosby et al. 2013), they do not allow for more focused questions related to the mechanotransduction mechanisms that regulate these changes. For instance, we have previously developed an in vitro model mimicking the matrix environment of the capsular ligament, with dissociated DRG neurons seeded on fabricated collagen gels (Zhang et al. 2016). Exposing that model to stretch similar to that sustained with injury, neuronal activation via upregulation of phosphorylated ERK (pERK) was found to occur at 11.7% strain, along with anomalous collagen realignment, suggesting that neuronal transcriptional activity and activation may be modulated, in part, by fiber-level kinematic changes of the collagen matrix (Zhang et al. 2016). Indeed, that neuron-collagen construct (NCC) has been used to identify the effects of collagen organization on pERK upregulation and modulation of nociceptive markers for loading of different magnitudes (Zhang et al. 2018). Specifically, integrin signaling has been studied in both NCCs and after painful facet joint injury in the rat, both of which lead to the upregulation of the pain neuromodulator substance P (Zhang et al. 2017b, 2018). In fact, inhibiting the $\alpha_2\beta_1$ integrin subunits prevents the loading-induced increases in substance P that are typical with painful loading (Zhang et al. 2017b). However, it is not known the role of integrin in the neuronal dysfunction pathways of innervated ligamentous tissue, or to what degree that dysfunction relates to macroscopic or fiber-level kinematics.

The main goal of this study was to evaluate the role of the $\alpha_2\beta_1$ integrin in neuronal dysfunction due to ligament stretch. This study leveraged the NCC model to determine what changes, if any, to the mechanical thresholds for neuronal dysfunction occur by inhibiting integrin binding, using the TC-I15 inhibitor for the β1 integrin subunit (Zhang et al. 2017b; Drobnik et al. 2019). Treated and untreated NCCs were loaded to failure, their macromechanics and local fiber kinematics measured, and evaluated for the expression and localization of extrasynaptic NMDA receptors. Overall, this approach begins to examine the downstream effects of macroscopic stretch on neuronal dysfunction, the role of integrin signaling in that neuronal dysfunction, and quantifies

macroscopic strain thresholds for upregulating expression of extrasynaptic NMDA receptors, which are useful indicators of neuronal dysregulation (Mesfin et al. 2012).

2 Methods

2.1 Neuron-collagen construct fabrication

Neuron-collagen constructs were prepared as previously described using rat tail Type I collagen (2 mg/mL; Corning, Inc.; Corning, NY) solution cast in 12-well plates, and incubated overnight at 37 °C (Fig. 1) (Zhang et al. 2016, 2018). The next day, DRG neurons were sterilely isolated from embryonic day 18 Sprague–Dawley rats (provided by the CNS Cell Culture Service Center of the Mahoney Institute of Neuroscience at Penn). DRGs were dissociated using a gentle dissociation protocol, and neurons were plated at a concentration of 3×10^5 cells/mL on the fabricated collagen gels, and incubated at 37 °C. Those neuron-seeded gels were cultured in neurobasal medium supplemented by 1% GlutaMAX, 2% B-27, 1% Fetal Bovine Serum, and 10 ng/mL 2.5S subunit nerve growth factor (all from Thermo Fisher Scientific; Waltham MA), along with 2 mg/mL glucose, 10 mM FdU, and 10 mM uridine (all from Sigma-Aldrich; St. Louis MO). After 2 days, culture media was replaced and the neurons were encapsulated in a second layer of collagen (~ 150μL) and incubated under the same conditions. A subset ($n = 8$) of NCCs was treated with an integrin β1 subunit inhibitor (100 μM; Tocris Bioscience, Minneapolis MN) in culture media 36 h before mechanical testing (Fig. 1), according to the dosing and timing that has previously been shown to prevent the increase in substance P that occurs with tensile loading in this same NCC system (Zhang et al. 2017b). At that same time point, untreated NCCs ($n = 12$) received only the culture media.

2.2 Mechanical testing and biomechanical analyses

At day 7 in vitro, separate groups of untreated ($n = 8$) and inhibitor-treated ($n = 4$) NCCs underwent biaxial stretch to failure using a planar testing machine (574LE2; TestResources; Shakopee, MN) (Fig. 1). NCCs were stamped into a cruciform shape (21 mm × 8 mm) and a marker grid was drawn on the gel surface using India ink to define regional elements to enable both local strain calculations and corresponding protein localization and expression measurements (Fig. 1). With the gel submerged in a phosphate-buffered saline solution (PBS) bath at 37 °C, each arm was secured to microclamps of the test machine equipped with load cells (500 g; ± 2mN sensitivity) (Fig. 1). Each arm was displaced by 12 mm to ensure the gel was stretched to an adequate degree to ensure its failure; the displacement rate of 3.8 mm/s simulated the strain rate across the facet capsule that produces tissue injury and persistent pain in vivo. (Panjabi et al. 1998; Stemper et al. 2005; Lee and Winkelstein 2009; Dong et al.

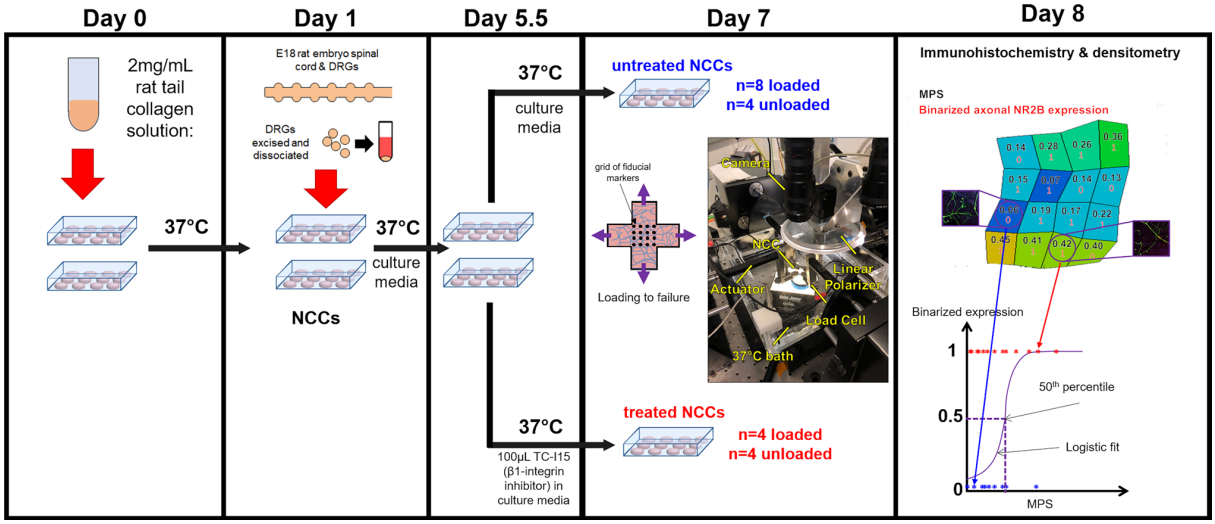

Fig. 1 Schematic overview outlining the overall study design and methods. Rat tail collagen solution self-assembled into gels before dissociated DRG neurons were plated on Day 1 to create neuron-collagen construct (NCC) gels. NCCs were cultured; 36 h before mechanical loading, a subset was exposed to β1-intgerin inhibitor in the culture media. On day-in-vitro (DIV) 7, both untreated and treated NCCs were labeled with markers to distinguish elements and loaded to failure. After exposure, NCCs were cultured for 24 h, and on Day 8 were fixed for immunohistochemical labeling of NR2B. Using densitometry analysis for each element, axonal NR2B expression was binarized as being either above or at control levels; those data were used in logistic regressions against maximum principal strain (MPS) to determine thresholds

2011, 2012; Crosby et al. 2014, 2015; Kartha et al. 2018; Singh et al. 2019). A high-speed camera system (Phantom-v9.1; Vision Research, Wayne NJ) acquired images (500fps) of each gel during loading to track marker positions and was also integrated with a polarized light system (Quinn and Winkelstein 2009; Quinn et al. 2010a) to obtain pixelwise collagen fiber alignment during loading. Force and displacement data (200 Hz) were synchronized with image acquisition and filtered with a 10-point moving average filter (Zhang et al. 2018). Subsets of untreated ($n=4$) and treated ($n=4$) gels that were placed in the warm bath but did not undergo any loading were included to serve as unloaded controls for the neuronal assays. After loading or the bath exposure, gels were transferred to a 12-well plate containing pre-warmed fresh culture medium supplemented with 1% Pen-Strep and incubated for 24 h before being fixed in 4% paraformaldehyde for immunohistochemical processing.

Force–displacement data for each arm were plotted for each NCC up to the gel failure, and the mechanical events of yield, first failure, and ultimate rupture were designated (Fig. 2). Yield was defined to occur at the first instance when the tangential stiffness decreased by 80% of the maximum tangential stiffness for any arm (Quinn et al. 2010a). First failure was the first detection of a peak force regardless of which arm it was established in; ultimate rupture occurred at the largest peak force of any of the arms during each test (Singh and Winkelstein 2018). Each failure event (first, ultimate rupture) was also confirmed visually from the high-speed images. Marker locations were digitized from the unloaded reference configuration and for each of the mechanical events; their positions for each event relative to the unloaded reference were tracked with ProAnalyst (Xcitex, Woburn MA) and elements were defined using the 4-point geometries defined by the markers (Fig. 1). Maximum principal strain (MPS) was calculated using the LS-DYNA finite element modeling software (LSTC, Livermore CA) for each element at ultimate rupture, and the elemental MPS was averaged for each gel.

In order to evaluate collagen fiber realignment during loading, a custom MATLAB script converted the digitized high-speed images and generated pixelwise fiber alignment maps of local collagen organization as previously described (Quinn and Winkelstein 2009, 2011a, b) (Fig. 2). Anomalous fiber realignment was identified using a vector correlation approach (Quinn and Winkelstein 2009, 2010). For each mechanical event (yield, first failure, ultimate rupture), 100 images before and 100 images after that event were extracted; the pixelwise vector correlation was calculated at intervals of every 20 frames based on the mean fiber direction and magnitude. The change in vector correlation coefficient was calculated for each pixel, and a region of connected 3 pixels × 3 pixels where the coefficient in each pixel decreased by 0.35 was defined as a region of anomalous fiber realignment (Quinn et al. 2010a).

In addition to evaluating fiber realignment across each gel, for each element defined by the fiducial markers, the mechanical event(s) at which anomalous realignment occurred was determined. Each element was classified as having no anomalous realignment detected, anomalous realignment at ultimate rupture, anomalous realignment before ultimate rupture, or anomalous realignment occurred regardless of mechanical event. If a single element exhibited anomalous fiber realignment occurring in multiple mechanical events, each incidence was recorded for the element.

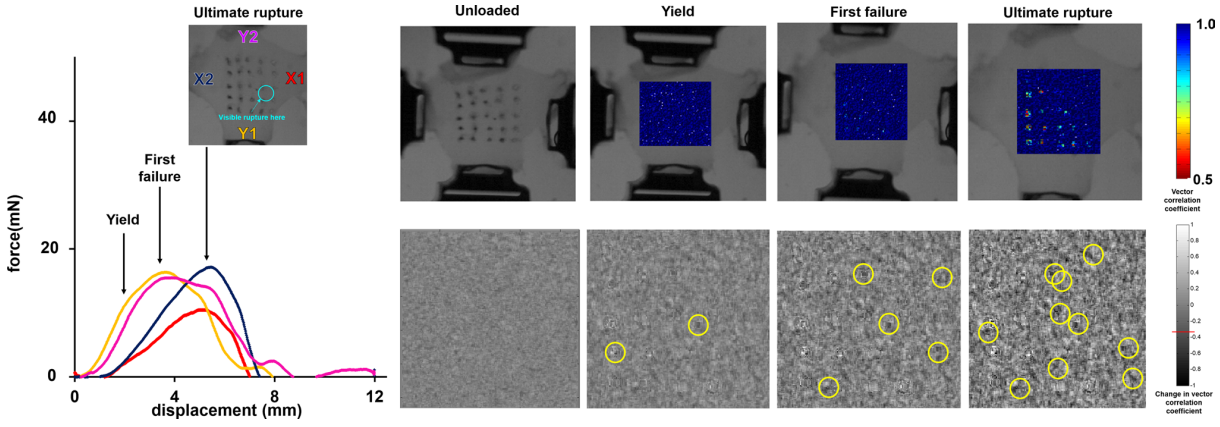

Fig. 2 For each NCC tested, force–displacement relationships were used to determine several relevant mechanical events including, the first instance of yield and failure, as well as the occurrence of ultimate rupture. At each event, optical imaging data from the 100 frames before and after were processed to determine changes in the local fiber alignment via the vector correlation coefficient (maps shown on top row) and to identify regions of anomalous fiber alignment (bottom row). Regions of anomalous realignment (circled in yellow) correspond to 3 × 3 pixels areas where the vector correlation coefficient decreases by more than 0.35 (Quinn and Winkelstein 2010; Quinn et al. 2010a)

2.3 Immunohistochemical assays and analyses

Twenty-four hours after loading, gels were immunolabeled for βIII-tubulin to visualize neuronal morphology and the NR2B subunit of the NMDA receptor, as a marker for neuron dysfunction (Mesfin et al. 2012). NCCs were blocked in 10% goat serum with 0.3% Triton-X PBS for 2 h at room temperature and then incubated overnight at 4 °C with chicken anti-βIII-tubulin (1:200; Sigma-Aldrich, St. Louis MO), and mouse anti-NR2B (1:500; Thermo Scientific. In addition, portions of each gel were immunolabeled for βIII-tubulin and the β1 integrin subunit to quantify the effects of the inhibitor. The next day, the fluorescent secondary antibodies goat-anti-chicken Alexa Fluor 488 (1:1000; Invitrogen, Carlsbad CA) and goat-anti-mouse Alexa Fluor 647 (1:1000; Invitrogen, Carlsbad CA) were applied to the gels for 2 h. After incubation, the cruciform arms were incubated with chicken anti-βIII-tubulin (1:200 Sigma-Aldrich, St. Louis MO) and rabbit anti-β1 integrin (1:200 Santa Cruz Biotechnology, Dallas TX). The secondary antibodies goat-anti-chicken Alexa Fluor 647 (1:1000; Invitrogen, Carlsbad CA), and goat-anti-rabbit Alexa Fluor 488 (1:1000; Invitrogen, Carlsbad CA) were applied for 2 h.

A Zeiss 710 confocal microscope (Carl Zeiss Microscopy, White Plains NY) was used to image regions of interest (2100×1800 pixels^2) corresponding to each element for each gel through a depth of 100 μm at every 5 μm using a 40× water immersion objective. The maximum projection was taken and using ImageJ (National Institutes of Health; Bethesda MD), the background was subtracted. Densitometry was performed using a custom MATLAB script to measure the percentages of positive pixels of colocalized βIII-tubulin with each of NR2B and β1 integrin (Rothman et al. 2010; Kartha et al. 2016). Those values for loaded gels were normalized to expression in unloaded, untreated control gels. Additionally, the percentage of pixels positive for axonal NR2B was determined by a separate custom MATLAB script that used the immunolabeled images of the gel by removing a 50×50 pixel^2 region centered around each soma and performing densitometry on the remaining axonal regions. The percentage of positive pixels for axonal NR2B was also normalized to unloaded, untreated gels.

2.4 Statistical analyses

Each of the force, displacement, and average elemental MPS for each gel at ultimate rupture was determined and separately compared between untreated and treated NCCs using student's t-tests for each biomechanical outcome. In addition, the amount of β1 integrin expression in each of the control and loaded gels was separately compared between treatment groups using student's t-tests. Force and displacement at ultimate rupture were compared using Student's t-tests with a 5% significance level (JMPv14, SAS, Cary NC).

Strain thresholds for upregulating axonal NR2B were also estimated by performing logistic regressions between the axonal NR2B and elemental MPS at ultimate rupture to define the relationship between macroscopic strain and the degree of neuronal dysfunction. (Fig. 1). Each NCC element was binarized based on its axonal NR2B expression level. The mean amount of axonal NR2B present in all of the elements of the unloaded gels from both treatment groups ($n = 185$) was used as the level of axonal NR2B expression evident in control unloaded conditions (value 0). For each element in the loaded NCCs, the extent of axonal NR2B was quantified and taken as present (value 1) and if that value exceeded the threshold for expression in the controls (Zhang et al. 2016). The binarized axonal data and elemental MPS values were fit (JMPv14, SAS, Cary NC) using separate logistic regressions for untreated and treated NCCs. Analysis of Covariance (ANCOVA) compared relationships between MPS and binarized axonal NR2B for each group; the 50th, 75th, and 90th percentiles were determined for each regression as an estimate of the strain threshold. In addition, elements were classified by the mechanical event when fiber realignment occurred and logistic regressions of binarized axonal NR2B expression and elemental MPS for both treatment groups were performed to distinguish between elements where anomalous realignment occurred and its effect on NR2B upregulation. These relationships were also compared using ANCOVA.

3 Results

3.1 Inhibiting β1 integrin reduces its expression

β1 integrin expression is generally evident both along the axon and within the soma of neurons (Fig. 3) in both the unloaded and loaded gels, regardless of treatment. Treating gels with the β1 integrin inhibitor TC-I15 decreases that expression regardless of whether they are exposed to loading or not (Fig. 3). In fact, integrin expression is decreased ($p < 0.001$) by 42% for unloaded controls and is decreased by 39.4% in gels loaded to failure (Fig. 3). While loading appears to increase integrin expression for both treated and untreated gels (Fig. 3), that increase is not significant ($p > 0.28$).

3.2 NCC macroscale and collagen fiber mechanics

Treatment with TC-I15 does not alter the mechanical response for NCCs loaded until their rupture (Fig. 4). At ultimate rupture, force is not different ($p = 0.12$) between untreated (24.9 ± 9.5 mN) and treated (29.9 ± 10.5 mN)

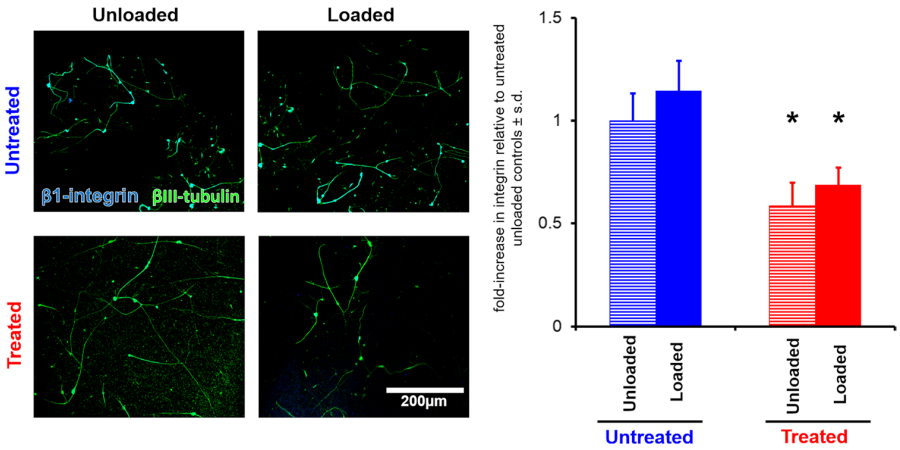

Fig. 3 Immunohistochemical co-labeling and quantification of β1-integrin (blue) and βIII-tubulin (green) in elements from both unloaded controls and NCCs loaded to failure. Treatment with the β1-integrin inhibitor TC-I15 reduces expression relative to untreated gels in both unloaded controls and gels loaded to failure (*$p<0.001$). Although loading appears to increase integrin expression in both groups, it is not significant ($p>0.28$)

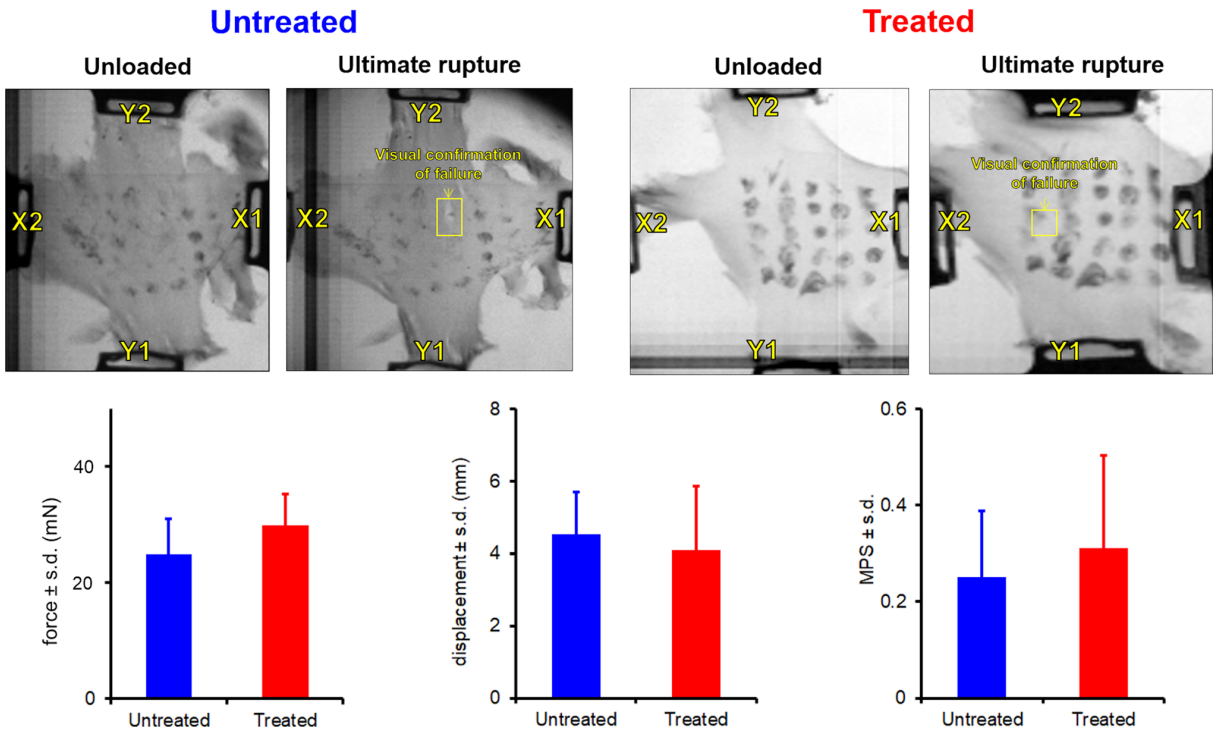

Fig. 4 Representative images of untreated and treated NCCs before loading (unloaded) and at ultimate rupture and summary mechanics at ultimate rupture. Both untreated and treated gels exhibit visible tears in the middle of the cruciform (labeled in yellow), corroborating detection of failure from the force–displacement profiles. At ultimate rupture, there is no difference in force ($p=0.12$), displacement ($p=0.44$), or average elemental maximum principal strain (MPS) ($p=0.78$) regardless of whether the gels were treated with TC-I15 or not

NCCs. Inhibiting the β1 integrin subunit does not alter the displacement at ultimate rupture (4.1 ± 1.8 mm) compared to untreated NCCs (4.5 ± 1.1 mm) ($p=0.44$), nor does treatment affect the average elemental MPS (0.31 ± 0.19) at ultimate rupture compared to untreated NCCs (0.25 ± 0.14) ($p=0.78$) (Fig. 4). In both groups, NCCs generally exhibit visible tears in the center region of the cruciform where the fiducial markers were placed (Fig. 4). In only two untreated NCCs and one treated NCC, visible failure occurred along the cruciform arm.

Anomalous collagen realignment is detected during loading in both the untreated and treated NCCs. In untreated NCC gels loaded to failure, 42 elements (34.7% of the 121 total untreated elements) do not have any realignment

events; yet, in 79 elements (65.3% of the 121 total untreated elements) from that group there is an anomalous fiber realignment event detected during any of the mechanical events. Of those elements (79 elements) experiencing anomalous fiber realignment during an event, 64.6% (51 elements) of them experience that anomalous realignment at ultimate rupture. In treated NCCs, 13 elements (20.3% of 64 total) do not experience an anomalous realignment event, and 51 (79.7%) experience at least one anomalous event during loading. Of those elements, 33 (51.6% of total treated elements) elements experience an event during ultimate rupture.

3.3 Neuronal NR2B expression and strain thresholds for its axonal expression

Axonal NR2B expression significantly increases with loading in both treatment groups ($p < 0.001$), with a 19.1 ± 4.5 fold-increase compared to unloaded untreated NCCs and a 13.4 ± 2.5 fold-increase compared to untreated unloaded NCCs in treated samples (Fig. 5). Across treatment groups, the fold-increase for loaded samples is 32.6% lower for treated samples than untreated samples ($p = 0.018$).

Using logistic regression, a 50th percentile strain threshold for upregulation of axonal NR2B is identified at 0.062 (Fig. 6). Inhibiting the β1 integrin subunit increases that strain threshold for axonal NR2B upregulation to an MPS of 0.071, with a significant increase over the untreated threshold ($p = 0.029$) (Fig. 6). Separating elements by the mechanical event when realignment occurs, strain percentile thresholds at all percentiles increase significantly ($p < 0.041$) with treatment except for those elements that do not experience realignment (Table 1). Although treatment decreases the strain thresholds for axonal NR2B upregulation in those elements, it is not changed from untreated levels ($p > 0.087$) (Table 1). Further, overall when considering those elements that experience a realignment event at any point during loading the threshold for axonal for NR2B upregulation increases with TC-I15 treatment but not significantly ($p > 0.148$) (Table 1).

4 Discussion

Macroscopic loading of the innervated capsular ligament transfers loads directly to the neurons embedded in the ligamentous matrix, as well as indirectly by integrin signaling mechanisms via collagen fiber deformations and reorganization that alter the matrix surrounding those neurons. Supraphysiological ligament loading can injure the primary afferents both via axonal and somata deformations (Zhang et al. 2018), as well as from secondary injury cascades that are mediated in part by calcium signaling (Schomberg et al. 2012). Since nonphysiological stretch induces both morphological (Tang-Schomer et al. 2010) and transcriptional (Hemphill et al. 2011) changes in afferents, macroscopic mechanical and fiber-level kinematic inputs were hypothesized to contribute to afferent dysfunction and injury via integrin signaling. Indeed, this study found that mechanical strain thresholds for the expression of axonal NR2B increases following inhibition of β1 integrin (Figs. 5, 6, Table 1). Because the DRG afferents that populate ligaments are unipolar neurons that do not generate dendrites characteristic of hippocampal or other CNS neurons (Basbaum et al. 2010), NR2B is a useful marker by proxy to assess neuronal dysfunction via the expression of extrasynaptic NMDA receptors.

Loading NCCs to failure increases NR2B expression in axons in both untreated and treated NCCs (Fig. 5). Axonal stretch injury is characterized by increases in intracellular calcium and upregulation of calpain (Bahr 2000; Laplaca and Prado 2010; Mesfin et al. 2012). Calcium ions are secondary messengers in a number of transcriptional and cellular signaling pathways that dictate nerve growth cones, axon

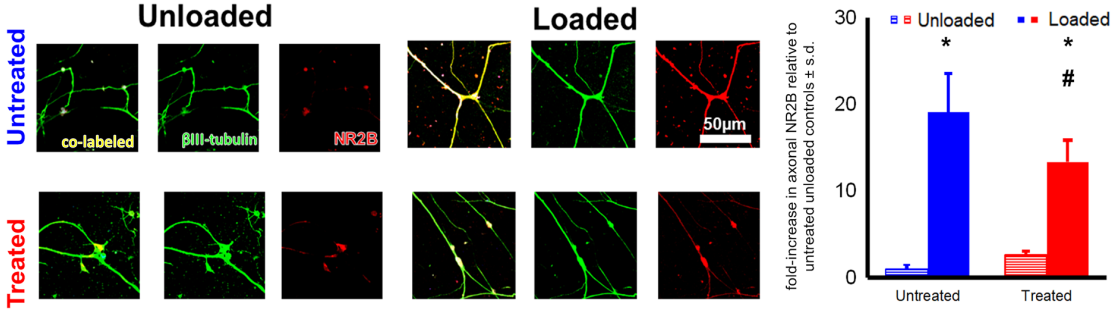

Fig. 5 Representative images of immunohistochemically co-labeled (yellow) NCCs for βIII-tubulin (green) and the NR2B subunit (red) for both untreated and treated groups that are unloaded and loaded to failure. Loading to failure increases the extent of axonal NR2B regardless of treatment, which is evident both in the images and through quantification of the colocalized βIII-tubulin and NR2B (*$p < 0.001$). In addition, the expression due to loading in the treated group is significantly lower than the expression in the matched loaded but untreated NCCs (#$p < 0.001$)

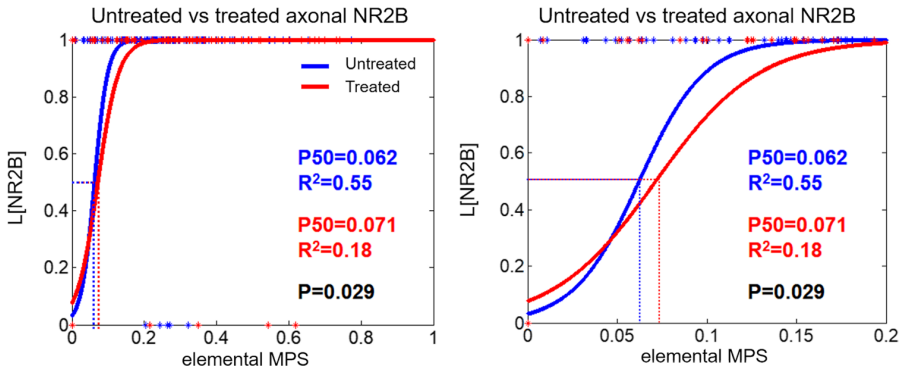

Fig. 6 Logistic regressions for binarized elemental axonal NR2B and elemental MPS are used to estimate strain thresholds for upregulation of axonal NR2B. The threshold is defined as the strain corresponding to 50th percentile (dotted line) of expression estimated by each logistic regression. Treatment with the β1-integrin inhibitor increases the threshold strain for upregulation from 0.062 to 0.071 ($p=0.029$). The right-side plot shows data with elemental strains below 0.20 in order to make the shift in the threshold more easily visualized

regeneration, and cell apoptosis (Chierzi et al. 2005; Henderson et al. 2005; Ahlgren et al. 2014; Carvajal et al. 2016) and are transported intracellularly by the NMDA receptor among other ion channels (Monnerie et al. 2010; Su et al. 2015). Under physiological conditions, NMDA receptors are primarily expressed in the somata where they maintain intracellular calcium concentrations (Ma and Hargreaves 2000; Groc et al. 2007; Ferrari et al. 2014). Ordinarily, the NR2A subunit is primarily found at the synapse (Li et al. 1998) and the NR2B subunit is localized to the axon (Groc et al. 2006, 2007; Petralia et al. 2009; Ladépêche et al. 2014). In fact, this localization is also evident in the unloaded NCCs, where NR2B primarily localizes to the neuron somata (Fig. 5). After macroscale gel stretch comparable to a painful injury (Lee et al. 2004a; Quinn and Winkelstein 2007; Lee and Winkelstein 2009; Dong et al. 2012), the sequestered NMDA receptors are transported to the synaptic or extrasynaptic regions (Fig. 5). Indeed, more NR2B is found in the extrasynaptic regions in loaded gels, with (13.4-fold increase) or without (19.1-fold increase) inhibitor treatment, than in unloaded, untreated gels (Fig. 5). The fact that more NR2B is observed in DRG axons in untreated gels loaded to failure suggests that stretch-activated β1 integrin can modulate the release of extrasynaptic NMDA. This assertion is supported by the similar levels of expression of extrasynaptic NR2B measured between treatment groups in the unloaded state (Fig. 5). Although the pathway dictating how activation of β1 integrin directs NMDA-NR2B transport is unclear, the receptor of the β1 family of integrins, reelin, has been speculated to participate in surface transport of NMDA receptors (Groc et al. 2007). Because reelin is also transiently expressed extracellularly by Schwann cells following peripheral nerve injury (Panteri et al. 2006; Pasten et al. 2015) and β1 integrin is ubiquitously expressed in both treatment groups in the current study (Fig. 3), reelin may regulate the increase in extrasynaptic NMDA receptors observed with NCC stretch.

Pretreating NCCs with the TC-I15 small molecule inhibitor for 36 h is effective in reducing β1 integrin expression in NCCs by 42% in the unloaded gels and 39.2% in the loaded gels (Fig. 3). It is not surprising that the treatment induces similar ($p<0.001$) decreases in β1 integrin expression across groups since the inhibitor competitively binds to the I-domain of the integrin subunits (Miller et al. 2009) regardless of loading. The TC-I15 inhibitor selectively binds to both the α2 and β1 subunits of integrin, both of which are receptors for type I collagen (Sabari et al. 2011; Zhang et al. 2017b) which is the primary component of our NCCs (Zhang et al. 2016, 2018). Further, type I collagen makes

Table 1 Elements are classified by anomalous realignment events that occur during loading, with strain thresholds for each event estimated for the 50th, 75th, and 90th percentiles of binarized elemental axonal NR2B expression

	Percentile	No event	Rupture*	Event besides rupture†	Any event
Untreated	50th	0.164	0.038	0.112	0.038
	75th	0.257	0.053	0.169	0.053
	90th	0.350	0.068	0.225	0.069
Treated	50th	0.107	0.049↑	0.169↑	0.040
	75th	0.163	0.069↑	0.267↑	0.057
	90th	0.218	0.088↑	0.363↑	0.074

Elements with no realignment detected at any mechanical event or all elements regardless of whether they experienced an event or not, do not exhibit significant differences in thresholds with treatment. However, elements where a realignment event occurs *only* at rupture, or with realignment *at any mechanical event* other than rupture, demonstrate a significant increase in strain threshold with treatment (*$p<0.01$; †$p<0.001$)

up a the majority of the ligament matrix, along with elastin, in both rat (Cavanaugh et al. 1989; Lee et al. 2006a, b) and human facet capsular ligaments (Yamashita et al. 1996; Little and Khalsa 2005). Because β1 integrin is shown to increase in dorsal root ganglia after painful facet capsule stretch (Zhang et al. 2017b) and in this NCC system after stretch (Zhang et al. 2017b) (Fig. 3), the reduced expression in β1 integrin with stretch following inhibition is not surprising (Fig. 3). Notably, while the inhibitor decreases expression of integrin, it does so nonselectively with no differences in localization observed between untreated and treated NCCs (Fig. 3). Interestingly, TC-I15 treatment reduces the level of *extrasynaptic* NR2B following loading (Fig. 5) suggesting that β1 integrin mediates the neuronal signals that transport NMDA receptors to the axons.

Because the strain thresholds for increased extrasynaptic NR2B (6.2% without inhibition and 7.1% with inhibition) overall are lower than the thresholds identified previously for pERK upregulation (11%) or pain (22%) (Dong et al. 2012; Zhang et al. 2016), transport of extrasynaptic NMDA receptors may be an initial step that may be required for the transcriptional changes associated with pain regulation from joint loading. In fact, the strains estimated here for inducing neuronal dysfunction through NR2B-expressing NMDA receptors are comparable to those strains sustained during physiologic but nonpainful (8%) loading of the ligament in vivo (Lee and Winkelstein 2009; Dong et al. 2012). However, examining responses more locally in the NCCs, it is evident that the increase in NR2B expression within individual elements of the NCCs corresponds to those elements that experience anomalous realignment (Table 1) (Quinn et al. 2010a; Zhang et al. 2016). Specifically, for those elements experiencing local anomalous collagen realignment at or before rupture the threshold for dysfunction (i.e., axonal NR2B exceeding 90% quantile in unloaded gels) is increased with integrin treatment (Fig. 5, Table 1). Conversely, the strain threshold for neuronal dysfunction in elements that *do not sustain any realignment* events at all is not different from the treatment group (Table 1); this finding supports the notion that collagen reorganization activates the β1 integrin subunit receptor that changes patterns of NR2B localization in afferent neurons (Conant et al. 2004). In fact, strains ranging from 30 to 75%, at strain rates similar to the ones experienced by the NCCs, have been reported to cause morphological changes and induce axonal stretch injury and degeneration in isolated axonal tracts in in vitro preparations (Tang-Schomer et al. 2010). The observed difference in estimated strain thresholds for elements undergoing collagen realignment during loading and those that do not (Fig. 6, Table 1) suggests that although macroscopic deformations of neurons and their surrounding matrix contribute to the upregulation of extrasynaptic NMDA, changes in extrasynaptic NMDA are more sensitive to the neuron–integrin–collagen interaction than to direct deformation of afferents.

Since neurons are far less stiff than the surrounding collagen and do not have contractile apparati like fibroblasts (Yang et al. 2015), the embedded neurons do not exert traction forces on the collagen fibers during macroscopic loading but are likely to be passive sensors in the ligamentous structure. As such, the lack of differences in the macroscopic metrics of failure force, displacement, and average MPS (Fig. 4) between both treatment groups is somewhat expected. Since neurons experience reaction forces through integrin signaling (Khalsa et al. 2000; Sun et al. 2019), it is likely that competitively inhibiting integrin receptors from binding to collagen fibers reduces the neuron's capability to sense collagen reorganization if it is sufficiently large during loading. Because the β1 integrin subunit binds through talin to the neuronal actin cytoskeleton and transmits force to the cytoskeleton due to deformations of the extracellular matrix (Michaluk et al. 2011; Sun et al. 2019), attenuating integrin-mediated interactions between afferents and collagen could increase the amount of tissue-level stretch required for neuronal dysfunction. Since there may be fewer of these intact tethers to the surrounding matrix to transmit force to the neuron (Sun et al. 2019), greater matrix deformation would be required to transmit the same amount of force, explaining the increase in strain thresholds that is observed in the treated NCCs (Table 1). Indeed, computational approaches modeling embedded nerve fibers in a collagen network which simulates this in vitro system find that increasing the network fiber volume concentration, which would increase the number of adhesions between the extracellular matrix and neuron, also increases the average strain across the neuron during macroscopic axial and transverse loading (Zarei et al. 2017b). NMDA receptors also contain mechanosensitive domains that provide feedback to the neuronal cytoskeleton (Wyszynski et al. 1997; Lei et al. 2001; Singh et al. 2012), with the C-terminus of the NR2B domain binding to the actin cytoskeleton indirectly through α-actinin (Wyszynski et al. 1997; Lei et al. 2001). However, unlike integrin, there are no reports suggesting NR2B binds to the extracellular matrix, further suggesting direct deformation of the neuron membrane as the activating stimulus for calcium influx mediated by NMDA receptors, as opposed to integrin signaling (Singh et al. 2012).

Since calcium signaling acts as a secondary messenger in mechanisms of both injury (Chierzi et al. 2005; Henderson et al. 2005; Monnerie et al. 2010) and repair (Li et al. 2007; Hunt et al. 2012), the increase in extrasynaptic NMDA observed with loading (Fig. 5) could be in response to increased intracellular calcium following injury (Zhou et al. 2013). The TC-I15 dose used here was selected because it has been shown to effectively inhibit substance P expression in this same NCC model

after macroscopic stretch producing strains sufficient to induce pain (Zhang et al. 2017b). It is possible that since substance P and extrasynaptic NMDA (Fig. 5) are both attenuated by inhibiting this integrin the increased calcium influx due to the upregulation of extrasynaptic NMDA may be upstream of the transcriptional changes that cause substance P upregulation (Liu et al. 1997) since receptor recruitment occurs on the order of hours after stimulation (Friedman et al. 2000). Of note, increases in intracellular calcium not only mediate nerve injury (Laplaca and Prado 2010) and regeneration (Chierzi et al. 2005), but also regulate pain mechanisms (Pezet et al. 2008). Taking that together with the fact that increased calcium signaling has also been observed in peripheral neurons in response to painful formalin injections in the rat hindpaw (McRoberts et al. 2001) and is increased in DRG neurons minutes after exposure to bacterial collagenase (Ita et al. 2020), suggests the increase in extrasynaptic NMDA receptors could be a precursor to sustained hypersensitivity and pain (Recio-Pinto and Castillo 2010).

Understanding the magnitude of load experienced by neurons embedded in the facet capsular ligament is a multiscale problem (Zarei et al. 2017b). Macroscopic loading to the ligament surrogate translates to fiber-level loading and local mechanics dictate the loading to the afferent neurons (Zarei et al. 2017b; Middendorf et al. 2021). As such, the microstructural organization and fiber-level mechanical properties of the ligament (or collagen matrix) are important in estimating the loads experienced by the neurons, and the extent to which integrin receptors translate fiber-level stresses to the neurons. For example, axonal strains have been shown to vary based on the heterogeneity of the collagen matrix with respect to its volume fraction and fiber orientation, whereby denser, aligned collagen networks increase the average axonal strain during axial loading (Yasodharababu and Nair 2020; Middendorf et al. 2021). The collagen organization in the ligamentous capsule of the spinal facet, for example, has been shown to differ across spinal levels and even within a single level, with a single capsular ligament exhibiting regions of randomly and preferentially oriented fibers (Quinn and Winkelstein 2011b; Ban et al. 2017; Claeson and Barocas 2017). Such variation in local microstructural organization, coupled with the complex loading on these joints due to the three-dimensional and coupled loading in the spine (Yoganandan et al. 1998; Duggal et al. 2005), places variable and complicated local loading on the resident neurons (Zarei et al. 2017a; Zhang et al. 2018). Such complex loading, together with the evidence of collagen fiber realignment and regional reorganization at loading conditions sufficiently below those for tissue damage (Quinn et al. 2007, 2010a; Quinn and Winkelstein 2008) has implications for altered functional outcomes in the axons, particularly given their vulnerability to shear injury (Cullen and Placa 2006) and the sensitivity of integrin subunits to shear loading rather than tensile loading (Chen et al. 1999).

Although failure mechanics were measured at the macroscopic level, and NMDA receptor upregulation following loading was evaluated at the cellular level (Fig. 4), changes in fiber kinematics were measured at the elemental level, as was strain (Fig. 6). As such, the thresholds for cellular dysfunction that are determined (Fig. 6, Table 1) are macroscopic and do not capture the local neuronal strains or the mechanical environment detected by integrins (Zarei et al. 2017b; Zhang et al. 2017a, b). Nevertheless, such data provide relative context about the loading experienced by the afferents, and these findings demonstrate that inhibiting integrin effects increases the neuron's tolerance (i.e., protects the neuron) for dysfunction resulting from injurious macroscopic stretch (Fig. 6, Table 1). Indeed, both computational models and finer resolution imaging techniques that better estimate cellular-scale loading are important for establishing microscale mechanical thresholds that injure afferents (Zhang et al. 2017a; Zarei et al. 2017b; Singh and Winkelstein 2021). The current findings highlight afferent dysfunction as a function of tissue-scale stretch and support its being mediated by integrin signaling as collagen fibers reorganize in response to stretch. The fact that inhibiting integrins elevates strain thresholds for NR2B upregulation also supports relationships between fiber-scale kinematics and afferent health and activity in innervated tissues similar to the facet capsular ligament.

Acknowledgements This work was funded by the NIH (#AT010326-07) and the Catherine Sharpe Foundation.

References

Ahlgren H, Bas-Orth C, Freitag HE et al (2014) The nuclear calcium signaling target, activating transcription factor 3 (ATF3), protects against dendrotoxicity and facilitates the recovery of synaptic transmission after an excitotoxic insult. J Biol Chem 289:9970–9982. https://doi.org/10.1074/jbc.M113.502914

Al-Jamal R, Harrison DJ (2008) Beta1 integrin in tissue remodelling and repair: from phenomena to concepts. Pharmacol Ther 120:81–101. https://doi.org/10.1016/j.pharmthera.2008.07.002

Bahr BA (2000) Integrin-type signaling has a distinct influence on NMDA-induced cytoskeletal disassembly. J Neurosci Res 59:827–832. https://doi.org/10.1002/(SICI)1097-4547(20000315)59:6%3c827::AID-JNR15%3e3.0.CO;2-Q

Ban E, Zhang S, Zarei V et al (2017) Collagen organization in facet capsular ligaments varies with spinal region and with ligament deformation. J Biomech Eng 139:071009. https://doi.org/10.1115/1.4036019

Basbaum AI, Bautista DM, Scherrer G, Julius D (2010) Cellular and molecular mechanisms of pain. NIH Public Access 139:267–284. https://doi.org/10.1016/j.cell.2009.09.028.Cellular

Carvajal FJ, Mattison HA, Cerpa W (2016) Role of NMDA receptor-mediated glutamatergic signaling in chronic and acute neuropathologies. Neural Plast. https://doi.org/10.1155/2016/2701526

Cavanaugh JM (2006) Pain generation in lumbar and cervical facet joints. J Bone Jt Surg 88:63. https://doi.org/10.2106/JBJS.E.01411

Cavanaugh JM, El-Bohy A, Hardy WN et al (1989) Sensory innervation of soft tissues of the lumbar spine in the rat. J Orthop Res 7:378–388. https://doi.org/10.1002/jor.1100070310

Cavanaugh JM, Ozaktay AC, Yamashita HT, King AI (1996) Lumbar facet pain: biomechanics, neuroanatomy and neurophysiology. J Biomech 29:1117–1129. https://doi.org/10.1016/0021-9290(96)00023-1

Chang YS, Kan HW, Hsieh YL (2019) Activating transcription factor 3 modulates protein kinase C epsilon activation in diabetic peripheral neuropathy. J Pain Res 12:317–326. https://doi.org/10.2147/JPR.S186699

Chen K-D, Li Y-S, Kim M et al (1999) Mechanotransduction in response to shear stress. J Biol Chem 274:18393–18400. https://doi.org/10.1074/jbc.274.26.18393

Chierzi S, Ratto GM, Verma P, Fawcett JW (2005) The ability of axons to regenerate their growth cones depends on axonal type and age, and is regulated by calcium, cAMP and ERK. Eur J Neurosci 21:2051–2062. https://doi.org/10.1111/j.1460-9568.2005.04066.x

Claeson AA, Barocas VH (2017) Planar biaxial extension of the lumbar facet capsular ligament reveals significant in-plane shear forces. J Mech Behav Biomed Mater 65:127–136. https://doi.org/10.1016/j.jmbbm.2016.08.019

Conant K, St. Hillaire C, Nagase H et al (2004) Matrix metalloproteinase 1 interacts with neuronal integrins and stimulates dephosphorylation of Akt. J Biol Chem 279:8056–8062. https://doi.org/10.1074/jbc.M307051200

Crosby ND, Weisshaar CL, Winkelstein BA (2013) Spinal neuronal plasticity is evident within 1 day after a painful cervical facet joint injury. Neurosci Lett 542:102–106. https://doi.org/10.1016/j.neulet.2013.03.019

Crosby ND, Gilliland TM, Winkelstein BA (2014) Early afferent activity from the facet joint after painful trauma to its capsule potentiates neuronal excitability and glutamate signaling in the spinal cord. Pain 155:1878–1887. https://doi.org/10.1016/j.pain.2014.06.019

Crosby ND, Weisshaar CL, Smith JR et al (2015) Burst and tonic spinal cord stimulation differentially activate gabaergic mechanisms to attenuate pain in a rat model of cervical radiculopathy. IEEE Trans Biomed Eng 62:1604–1613. https://doi.org/10.1109/TBME.2015.2399374

Cullen DK, Placa MCLA (2006) Neuronal response to high rate shear deformation depends on heterogeneity of the local strain field. J Neurotrauma 23:1304–1319

Dina OA, Parada CA, Yeh J et al (2004) Integrin signaling in inflammatory and neuropathic pain in the rat. Eur J Neurosci 19:634–642. https://doi.org/10.1111/j.1460-9568.2003.03169.x

Dina OA, Hucho T, Yeh J et al (2005) Primary afferent second messenger cascades interact with specific integrin subunits in producing inflammatory hyperalgesia. Pain 115:191–203. https://doi.org/10.1016/j.pain.2005.02.028

Dong L, Guarino BB, Jordan-Sciutto KL, Winkelstein BA (2011) Activating transcription factor 4, a mediator of the integrated stress response, is increased in the dorsal root ganglia following painful facet joint distraction. Neuroscience 193:377–386. https://doi.org/10.1016/j.neuroscience.2011.07.059

Dong L, Quindlen JC, Lipschutz DE, Winkelstein BA (2012) Whiplash-like facet joint loading initiates glutamatergic responses in the DRG and spinal cord associated with behavioral hypersensitivity. Brain Res 1461:51–63. https://doi.org/10.1016/j.brainres.2012.04.026

Drobnik J, Pietrucha K, Janczar K et al (2019) Intra-cerebral implantation of a variety of collagenous scaffolds with nervous embryonic cells. Exp Ther Med. https://doi.org/10.3892/etm.2019.8116

Duggal N, Chamberlain RH, Park SC et al (2005) Unilateral cervical facet dislocation: biomechanics of fixation. Spine 30:E164–E168. https://doi.org/10.1097/01.brs.0000157418.20900.a1

Emsley J, Knight CG, Farndale RW et al (2000) Structural basis of collagen recognition by integrin α2β1. Cell 101:47–56. https://doi.org/10.1016/S0092-8674(00)80622-4

Ferrari LF, Lotufo CM, Araldi D et al (2014) Inflammatory sensitization of nociceptors depends on activation of NMDA receptors in DRG satellite cells. Proc Natl Acad Sci USA 111:18363–18368. https://doi.org/10.1073/pnas.1420601111

Friedman HV, Bresler T, Garner CC, Ziv NE (2000) Assembly of new individual excitatory synapses: time course and temporal order of synaptic molecule recruitment. Neuron 27:57–69. https://doi.org/10.1016/s0896-6273(00)00009-x

Gladding CM, Raymond LA (2011) Mechanisms underlying NMDA receptor synaptic/extrasynaptic distribution and function. Mol Cell Neurosci 48:308–320. https://doi.org/10.1016/j.mcn.2011.05.001

Groc L, Heine M, Cousins SL et al (2006) NMDA receptor surface mobility depends on NR2A-2B subunits. Proc Natl Acad Sci USA 103:18769–18774. https://doi.org/10.1073/pnas.0605238103

Groc L, Choquet D, Stephenson FA et al (2007) NMDA receptor surface trafficking and synaptic subunit composition are developmentally regulated by the extracellular matrix protein reelin. J Neurosci 27:10165–10175. https://doi.org/10.1523/JNEUROSCI.1772-07.2007

Grossman SD, Wolfe BB, Yasuda RP, Wrathall JR (2000) Changes in NMDA receptor subunit expression in response to contusive spinal cord injury. J Neurochem 75:174–184

Hamidi H, Ivaska J (2018) Every step of the way: integrins in cancer progression and metastasis. Nat Rev Cancer. https://doi.org/10.1038/s41568-018-0038-z

Hemphill MA, Dabiri BE, Gabriele S et al (2011) A possible role for integrin signaling in diffuse axonal injury. PLoS ONE. https://doi.org/10.1371/journal.pone.0022899

Hemphill MA, Dauth S, Yu CJ et al (2015) Traumatic brain injury and the neuronal microenvironment: a potential role for neuropathological mechanotransduction. Neuron 85:1177–1192. https://doi.org/10.1016/j.neuron.2015.02.041

Henderson FC, Geddes JF, Vaccaro AR et al (2005) Stretch-associated injury in cervical spondylotic myelopathy: New concept and review. Neurosurgery 56:1101–1112. https://doi.org/10.1227/01.NEU.0000157929.85251.7C

Hill CS, Coleman MP, Menon DK (2016) Traumatic axonal injury: mechanisms and translational opportunities. Trends Neurosci 39:311–324. https://doi.org/10.1016/j.tins.2016.03.002

Hoffman BD, Grashoff C, Schwartz MA (2011) Dynamic molecular processes mediate cellular mechanotransduction. Nature 475:316–323. https://doi.org/10.1038/nature10316

Hunt D, Raivich G, Anderson PN (2012) Activating transcription factor 3 and the nervous system. Front Mol Neurosci 5:1–17. https://doi.org/10.3389/fnmol.2012.00007

Hynes RO (2002) Integrins: bidirectional, allosteric signaling machines in their roles as major adhesion receptors. Cell 110:673–687. https://doi.org/10.1016/S0092-8674(02)00971-6

Ita ME, Ghimire P, Welch RL et al (2020) Intra-articular collagenase in the spinal facet joint induces pain, DRG neuron dysregulation and increased MMP-1 absent evidence of joint destruction. Sci Rep 10:1–15. https://doi.org/10.1038/s41598-020-78811-3

Janoštiak R, Pataki AC, Brábek J, Rösel D (2014) Mechanosensors in integrin signaling: the emerging role of p130Cas. Eur J Cell Biol 93:445–454. https://doi.org/10.1016/j.ejcb.2014.07.002

Kallakuri S, Li Y, Chen C, Cavanaugh JM (2012) Innervation of cervical ventral facet joint capsule: histological evidence. World J Orthop 3:10. https://doi.org/10.5312/wjo.v3.i2.10

Kartha S, Zhou T, Granquist EJ, Winkelstein BA (2016) Development of a rat model of mechanically induced tunable pain and associated temporomandibular joint responses. J Oral Maxillofac Surg 74:54.e1-54.e10. https://doi.org/10.1016/j.joms.2015.09.005

Kartha S, Bulka BA, Stiansen NS et al (2018) Repeated high rate facet capsular stretch at strains that are below the pain threshold induces pain and spinal inflammation with decreased ligament strength in the rat. J Biomech Eng 140:1–8. https://doi.org/10.1115/1.4040023

Khalsa PS, Zhang C, Sommerfeldt D, Hadjiargyrou M (2000) Expression of integrin α2β1 in axons and receptive endings of neurons in rat, hairy skin. Neurosci Lett 293:13–16. https://doi.org/10.1016/S0304-3940(00)01482-8

Kong F, Li Z, Parks WM et al (2013) Cyclic mechanical reinforcement of integrin-ligand interactions. Mol Cell 49:1060–1068. https://doi.org/10.1016/j.molcel.2013.01.015

Kras JV, Tanaka K, Gilliland TM, Winkelstein BA (2013) An anatomical and immunohistochemical characterization of afferents innervating the C6–C7 facet joint after painful joint loading in the rat. Spine 38:E325–E331. https://doi.org/10.1097/BRS.0b013e318285b5bb

Ladépêche L, Dupuis JP, Groc L (2014) Surface trafficking of NMDA receptors: gathering from a partner to another. Semin Cell Dev Biol 27:3–13. https://doi.org/10.1016/j.semcdb.2013.10.005

Lal H, Verma SK, Smith M et al (2007) Stretch-induced MAP kinase activation in cardiac myocytes: differential regulation through β1-integrin and focal adhesion kinase. J Mol Cell Cardiol 43:137–147. https://doi.org/10.1016/j.yjmcc.2007.05.012

Laplaca MC, Prado GR (2010) Neural mechanobiology and neuronal vulnerability to traumatic loading. J Biomech 43:71–78. https://doi.org/10.1016/j.jbiomech.2009.09.011

Laplaca MC, Thibault LE (1998) Dynamic mechanical deformation of neurons triggers an acute calcium response and cell injury involving the N-methyl-D-aspartate glutamate receptor. J Neurosci Res 229:220–229

Lee KE, Winkelstein BA (2009) Joint distraction magnitude is associated with different behavioral outcomes and substance P levels for cervical facet joint loading in the rat. J Pain 10:436–445. https://doi.org/10.1016/j.jpain.2008.11.009

Lee KE, Davis MB, Mejilla RM, Winkelstein BA (2004a) In vivo cervical facet capsule distraction: mechanical implications for whiplash and neck pain. Stapp Car Crash J 48:373–395

Lee KE, Thinnes JH, Gokhin DS, Winkelstein BA (2004b) A novel rodent neck pain model of facet-mediated behavioral hypersensitivity : implications for persistent pain and whiplash injury. J Neurosci Methods 137:151–159. https://doi.org/10.1016/j.jneumeth.2004.02.021

Lee K, Gupta M, Winkelstein B (2006a) In vivo facet capsule failure in a rat model: Implications for whiplash & facet-mediated neck pain. J Biomech 39:S148. https://doi.org/10.1016/s0021-9290(06)83497-4

Lee KE, Franklin AN, Davis MB, Winkelstein BA (2006b) Tensile cervical facet capsule ligament mechanics: failure and subfailure responses in the rat. J Biomech 39:1256–1264. https://doi.org/10.1016/j.jbiomech.2005.03.018

Lei S, Czerwinska E, Czerwinski W et al (2001) Regulation of NMDA receptor activity by F-actin and myosin light chain kinase. J Neurosci 21:8464–8472

Li JH, Wang YH, Wolfe BB et al (1998) Developmental changes in localization of NMDA receptor subunits in primary cultures of cortical neurons. Eur J Neurosci 10:1704–1715

Li W-C, Cooke T, Sautois B et al (2007) Axon and dendrite geography predict the specificity of synaptic connections in a functioning spinal cord network. Neural Dev 2:17. https://doi.org/10.1186/1749-8104-2-17

Little J, Khalsa P (2005) Material properties of the human lumbar facet joint capsule. J Biomech Eng 127:15–24. https://doi.org/10.1016/j.pestbp.2011.02.012.Investigations

Liu H, Mantyh PW, Basbaum AI (1997) NMDA-receptor regulation of substance P release from primary afferent nociceptors. Nature 386:721–724

Ma QP, Hargreaves RJ (2000) Localization of N-methyl-D-aspartate NR2B subunits on primary sensory neurons that give rise to small-caliber sciatic nerve fibers in rats. Neuroscience 101:699–707. https://doi.org/10.1016/S0306-4522(00)00419-X

Malik-Hall M, Dina OA, Levine JD (2005) Primary afferent nociceptor mechanisms mediating NGF-induced mechanical hyperalgesia. Eur J Neurosci 21:3387–3394. https://doi.org/10.1111/j.1460-9568.2005.04173.x

McRoberts JA, Coutinho SV, Marvizón JCG et al (2001) Role of peripheral N-methyl-D-aspartate (NMDA) receptors in visceral nociception in rats. Gastroenterology 120:1737–1748. https://doi.org/10.1053/gast.2001.24848

Mesfin MN, von Reyn CR, Mott RE et al (2012) In vitro stretch injury induces time- and severity-dependent alterations of STEP phosphorylation and proteolysis in neurons. J Neurotrauma 29:1982–1998. https://doi.org/10.1089/neu.2011.2253

Michaluk P, Wawrzyniak M, Alot P et al (2011) Influence of matrix metalloproteinase MMP-9 on dendritic spine morphology. J Cell Sci 124:3369–3380. https://doi.org/10.1242/jcs.090852

Middendorf JM, Ita ME, Winkelstein BA, Barocas VH (2021) Local tissue heterogeneity may modulate neuronal responses via altered axon strain fields: insights about innervated joint capsules from a computational model. Biomech Model Mechanobiol 20:2269–2285. https://doi.org/10.1007/s10237-021-01506-9

Miller MW, Basra S, Kulp DW et al (2009) Small-molecule inhibitors of integrin α2β1 that prevent pathological thrombus formation via an allosteric mechanism. Proc Natl Acad Sci U S A 106:719–724. https://doi.org/10.1073/pnas.0811622106

Monnerie H, Tang-Schomer MD, Iwata A et al (2010) Dendritic alterations after dynamic axonal stretch injury in vitro. Exp Neurol 224:415–423. https://doi.org/10.1016/j.expneurol.2010.05.001

Müller U (2004) Integrins and extracellular matrix in animal models. Handb Exp Pharmacol. https://doi.org/10.1007/978-3-540-68170-0_8

Panjabi MM, Cholewicki J, Nibu K et al (1998) Capsular ligament stretches during in vitro whiplash simulations. J Spinal Disord 11:227–232

Panteri R, Mey J, Zhelyaznik N et al (2006) Reelin is transiently expressed in the peripheral nerve during development and is upregulated following nerve crush. Mol Cell Neurosci 32:133–142. https://doi.org/10.1016/j.mcn.2006.03.004

Pasten C, Cerda J, Jausoro I et al (2015) ApoER2 and reelin are expressed in regenerating peripheral nerve and regulate Schwann cell migration by activating the Rac1 GEF protein, Tiam1. Mol Cell Neurosci 69:1–11. https://doi.org/10.1016/j.mcn.2015.09.004

Petralia RS, Al-Hallaq RA, Wenthold RJ (2009) Trafficking and targeting of NMDA receptors. Biol NMDA Recept 4:1–42

Pezet S, Marchand F, D'Mello R et al (2008) Phosphatidylinositol 3-kinase is a key mediator of central sensitization in painful inflammatory conditions. J Neurosci 28:4261–4270. https://doi.org/10.1523/JNEUROSCI.5392-07.2008

Quinn KP, Winkelstein BA (2007) Cervical facet capsular ligament yield defines the threshold for injury and persistent joint-mediated neck pain. J Biomech 40:2299–2306. https://doi.org/10.1016/j.jbiomech.2006.10.015

Quinn KP, Winkelstein BA (2008) Altered collagen fiber kinematics define the onset of localized ligament damage during loading. J Appl Physiol 105:1881–1888. https://doi.org/10.1152/japplphysiol.90792.2008

Quinn KP, Winkelstein BA (2009) Vector correlation technique for pixel-wise detection of collagen fiber realignment during injurious tensile loading. J Biomed Opt 14:054010-1–10. https://doi.org/10.1117/1.3227037

Quinn KP, Winkelstein BA (2010) Full field strain measurements of collagenous tissue by tracking fiber alignment through vector correlation. J Biomech 43:2637–2640. https://doi.org/10.1016/j.jbiomech.2010.05.008

Quinn KP, Winkelstein BA (2011a) Preconditioning is correlated with altered collagen fiber alignment in ligament. J Biomech Eng 133:64506. https://doi.org/10.1115/1.4004205

Quinn KP, Winkelstein BA (2011b) Detection of altered collagen fiber alignment in the cervical facet capsule after whiplash-like joint retraction. Ann Biomed Eng 39:2163–2173. https://doi.org/10.1007/s10439-011-0316-3

Quinn KP, Lee KE, Ahaghotu CC, Winkelstein BA (2007) Structural changes in the cervical facet capsular ligament: potential contributions to pain following subfailure loading. Proc 51st Stapp Car Crash J 51:169–187

Quinn KP, Bauman JA, Crosby ND, Winkelstein BA (2010a) Anomalous fiber realignment during tensile loading of the rat facet capsular ligament identifies mechanically induced damage and physiological dysfunction. J Biomech 43:1870–1875. https://doi.org/10.1016/j.jbiomech.2010.03.032

Quinn KP, Dong L, Golder FJ, Winkelstein BA (2010b) Neuronal hyperexcitability in the dorsal horn after painful facet joint injury. Pain 151:414–421. https://doi.org/10.1016/j.pain.2010.07.034

Recio-Pinto E, Castillo C (2010) Peripheral N-methyl-D-aspartate receptors as possible targets for chronic pain treatment. Tech Reg Anesth Pain Manage 14:48–58. https://doi.org/10.1053/j.trap.2010.04.001

Rothman SM, Nicholson KJ, Winkelstein BA (2010) Time-dependent mechanics and measures of glial activation and behavioral sensitivity in a rodent model of radiculopathy. J Neurotrauma 27:803–814. https://doi.org/10.1089/neu.2009.1045

Sabari J, Lax D, Connors D et al (2011) Fibronectin matrix assembly suppresses dispersal of glioblastoma cells. PLoS ONE 6:e24810. https://doi.org/10.1371/journal.pone.0024810

Schomberg D, Ahmed M, Miranpuri G et al (2012) Neuropathic pain: role of inflammation, immune response, and ion channel activity in central injury mechanisms. Ann Neurosci 19:125–132. https://doi.org/10.5214/ans.0972.7531.190309

Singh S, Winkelstein BA (2018) The neuronal injury marker ATF3 is more sensitive to shear strain than maximum principal strain for DRG neurons under stretch in collagen gels regardless of collagen alignment. 8th World Congr. Biomech. Abstract #2754

Singh S, Winkelstein BA (2021) Changes in fiber level strains & calcium activity after exposure to bacterial collagenase in neuron collagen constructs mimicking ligaments suggests possible mechanisms for pain associated with joint degeneration. Summer Biomech Bioeng Biotransport Conf 2021:17–18

Singh P, Doshi S, Spaethling JM et al (2012) N-methyl-D-aspartate receptor mechanosensitivity is governed by C terminus of NR2B subunit. J Biol Chem 287:4348–4359. https://doi.org/10.1074/jbc.M111.253740

Singh S, Kartha S, Bulka BA et al (2019) Physiologic facet capsule stretch can induce pain & upregulate matrix metalloproteinase-3 in the dorsal root ganglia when preceded by a physiological mechanical or nonpainful chemical exposure. Clin Biomech. https://doi.org/10.1016/j.clinbiomech.2018.01.009

Stemper BD, Yoganandan N, Gennarelli TA, Pintar FA (2005) Localized cervical facet joint kinematics under physiological and whiplash loading. J Neurosurg Spine 3:471–476. https://doi.org/10.3171/spi.2005.3.6.0471

Stukel JM, Willits RK (2016) Mechanotransduction of neural cells through cell-substrate interactions. Tissue Eng Part B 22:173–182. https://doi.org/10.1089/ten.teb.2015.0380

Su J, Gao T, Shi T et al (2015) Phenotypic changes in dorsal root ganglion and spinal cord in the collagen antibody-induced arthritis mouse model. J Comp Neurol 523:1505–1528. https://doi.org/10.1002/cne.23749

Sun Z, Guo SS, Fässler R (2016) Integrin-mediated mechanotransduction. J Cell Biol. https://doi.org/10.1083/jcb.201609037

Sun Z, Costell M, Fässler R (2019) Integrin activation by talin, kindlin and mechanical forces. Nat Cell Biol 21:25–31. https://doi.org/10.1038/s41556-018-0234-9

Tang-Schomer MD, Patel AR, Baas PW, Smith DH (2010) Mechanical breaking of microtubules in axons during dynamic stretch injury underlies delayed elasticity, microtubule disassembly, and axon degeneration. FASEB J 24:1401–1410. https://doi.org/10.1096/fj.09-142844

Tang-Schomer MD, Johnson VE, Baas PW et al (2012) Partial interruption of axonal transport due to microtubule breakage accounts for the formation of periodic varicosities after traumatic axonal injury. Exp Neurol 233:364–372. https://doi.org/10.1016/j.expneurol.2011.10.030

Tekieh T, Shahzadi S, Rafii-Tabar H, Sasanpour P (2016) Are deformed neurons electrophysiologically altered? A simulation study. Curr Appl Phys 16:1413–1417. https://doi.org/10.1016/j.cap.2016.07.012

Unezaki S, Sasaki A, Mabuchi T et al (2012) Involvement of Tyr1472 phosphorylation of NMDA receptor NR2B subunit in postherpetic neuralgia in model mice. Mol Pain 8:1. https://doi.org/10.1186/1744-8069-8-59

Wiesner S, Legate KR, Fässler R (2005) Integrin-actin interactions. Cell Mol Life Sci 62:1081–1099. https://doi.org/10.1007/s00018-005-4522-8

Wigerblad G, Huie JR, Yin HZ et al (2017) Inflammation-induced GluA1 trafficking and membrane insertion of Ca 2+ permeable AMPA receptors in dorsal horn neurons is dependent on spinal tumor necrosis factor, PI3 kinase and protein kinase A. Exp Neurol 293:144–158. https://doi.org/10.1016/j.expneurol.2017.04.004

Wu X, Reddy DS (2012) Integrins as receptor targets for neurological disorders. Pharmacol Ther 134:68–81. https://doi.org/10.1016/j.pharmthera.2011.12.008

Wyszynski M, Lin J, Rao A et al (1997) Competitive binding of α-actinin and calmodulin to the NMDA receptor. Nature 385:439–442. https://doi.org/10.1038/385439a0

Yamashita T, Minaki Y, Ozaktay AC et al (1996) A morphological study of the fibrous capsule of the human lumbar facet joint. Spine 21:538–543

Yang TH, Thoreson AR, Gingery A et al (2015) Collagen gel contraction as a measure of fibroblast function in an animal model of subsynovial connective tissue fibrosis. J Orthop Res 33:668–674. https://doi.org/10.1002/jor.22835

Yasodharababu M, Nair AK (2020) A multiscale model to predict neuronal cell deformation with varying extracellular matrix stiffness and topography. Cell Mol Bioeng 13:229–245. https://doi.org/10.1007/s12195-020-00615-2

Yoganandan N, Pintar FA, Klienberger M (1998) Cervical spine vertebral and facet joint kinematics under whiplash. J Biomech Eng 120:305. https://doi.org/10.1115/1.2798318

Yoganandan N, Pintar FA, Zhang J et al (2008) Upper neck forces and moments and cranial angular accelerations in lateral impact. Ann Biomed Eng 36:406–414. https://doi.org/10.1007/s10439-007-9422-7

Zarei V, Liu CJ, Claeson AA et al (2017a) Image-based multiscale mechanical modeling shows the importance of structural heterogeneity in the human lumbar facet capsular ligament.

Biomech Model Mechanobiol 16:1425–1438. https://doi.org/10.1007/s10237-017-0896-4

Zarei V, Zhang S, Winkelstein BA, Barocas VH (2017b) Tissue loading and microstructure regulate the deformation of embedded nerve fibres: predictions from single-scale and multiscale simulations. J R Soc Interface 14:20170326

Zhang S, Cao X, Stablow AM et al (2016) Tissue strain reorganizes collagen with a switchlike response that regulates neuronal extracellular signal-regulated kinase phosphorylation in vitro: implications for ligamentous injury and mechanotransduction. J Biomech Eng 138:021013. https://doi.org/10.1115/1.4031975

Zhang S, Zarei V, Winkelstein BA, Barocas VH (2017a) Multiscale mechanics of the cervical facet capsular ligament, with particular emphasis on anomalous fiber realignment prior to tissue failure. Biomech Model Mechanobiol 17:133–145. https://doi.org/10.1007/s10237-017-0949-8

Zhang S, Zhao E, Winkelstein BA (2017b) A nociceptive role for integrin signaling in pain after mechanical injury to the spinal facet capsular ligament. Ann Biomed Eng 45:2813–2825. https://doi.org/10.1007/s10439-017-1917-2

Zhang S, Singh S, Winkelstein BA (2018) Collagen organization regulates stretch-initiated pain-related neuronal signals in vitro: implications for structure-function relationships in innervated ligaments. J Orthop Res 36:770–777. https://doi.org/10.1002/jor.23657

Zhou X, Hollern D, Liao J et al (2013) NMDA receptor-mediated excitotoxicity depends on the coactivation of synaptic and extrasynaptic receptors. Cell Death Dis 4:1–11. https://doi.org/10.1038/cddis.2013.82

Publisher's Note Springer Nature remains neutral with regard to jurisdictional claims in published maps and institutional affiliations.